Journal of Applied Surfaces and Interfaces 4 (1-3) (2018) 1-8

Journal homepage: http://revues.imist.ma/?journal=jasi

ISSN: 2550-4800

https://doi.org/10.48442/IMIST.PRSM/jasi-v4i1-3.11273

JASI JOURNAL OF APPLIED SURFACES AND INTERFACES

Structure and some physical properties of sodium ion conducting glasses inside the Na_2O-Na_2WO_4-TiO_2-P_2O_5 system

H. Es-soufi [1], H. Bih [2], L. Bih [1], M. Azrour [3], B. Manoun [4,5], P. Lazor [6].

[1] *Equipe de Physico-Chimie de la Matière Condensée, PCMC, Faculté des Sciences de Meknes. Université Moulay Ismail, Morocco.*
[2] *Faculté polydisciplinaire de Taza, Université Sidi Mohamed ben Abdellah, Fes, Morocco.*
[3] *Equipe Sciences des matéraux, FST-Errachidia, Université Moulay Ismail, Morocco.*
[4] *Laboratoire des Sciences des Matériaux, des Milieux et de la Modélisation (LS3M), Univ Hassan 1er, 26000, Morocco*
[5] *Materials Science and Nano-engineering Department, Mohammed VI Polytechnic University, Ben Guerir, Morocco.*
[6] *Department of Earth Sciences, Uppsala University, SE-752 36, Uppsala, Sweden.*

Received 27 January 2018; Revised 17 August 2018; Accepted 04 September 2018.

Abstract : *A melt-quenched method is used to prepare homogeneous glasses inside the $20Na_2O$-$(50-x)Na_2WO_4$-$xTiO_2$-$30P_2O_5$ ($0\leq x\leq 25$ mol%) system. The amorphous and glassy states of the glasses are evidenced by X-Ray diffraction and differential scanning calorimetry (DSC) analysis, respectively. The glasses were found to be colorless. Some physical parameters for the glasses such as density, molar volume and glass transition temperature (T_g) are determined and depended strongly on the chemical composition of the glasses. The density and T_g showed the decrease and the increase with TiO_2 content, respectively. Infrared spectroscopy (IR) and Raman spectroscopy are used to characterize their structural approach. These both techniques have allowed the identification of different phosphate structural units mainly pyrophosphate and metaphosphate in their structure. From the absorption edge studies, the values of the optical band gap (E_g) and Urbach energy (ΔE) were evaluated. The optical band gap was found to depend on the glass composition and its value decreased as the content of TiO_2 increases. The σ_{dc} conductivity of the glasses is determined and it followed an Arrhenius behavior as a function of temperature. These electrical data are analyzed by the modulus formalism.*

Keywords: *Phosphate glasses; DSC; IR; Optical properties; electrical Conductivity.*

1. Introduction

Phosphate glasses are related to amorphous materials built based on the former oxide P_2O_5. One of the great drawbacks of these materials is their weak chemical stability. Since the date where scientists had formulate water-resist glasses by adding to the composition some oxides such as Fe_2O_3, Al_2O_3, ZnO [1,2], these glasses had found applications in several fields of materials science [3-8]. In previous works [9-13], it is found that the presence of titanium and tungsten oxides in phosphate glasses improves their chemical durability, thermal stability and other physical properties. This increase of stability is due to the incorporation of TiO_x or WO_x structural units into the phosphate structural network [11]. Recently [13,14], it is reported that lithium phosphate glasses containing Li_2WO_4 and TiO_2 showed good chemical stability and were free from W^{5+} and Ti^{3+} reduced species. Also these materials contained high lithium ratio with very low electronic conductivity. These properties could anticipate the possibility of their use as solid electrolytes. Actually, the development of sodium batteries has focused the interest of scientists to develop sodium conductors as solid electrolytes. It appeared that sodium phosphate glasses could be promising glassy electrolytes for the development of technologically and biologically important materials. In this point of view, we have studied new sodium phosphate glassy materials containing both TiO_2 and Na_2WO_4. The glasses inside the Na_2O-Na_2WO_4-TiO_2-P_2O_5 system are studied. The effect of the substitution of Na_2WO_4 by TiO_2 on the structure and the thermal, optical and electrical properties of these glasses are reported.

2. Experimental procedure

The $20Na_2O$-$(50-x)Na_2WO_4$-$xTiO_2$-$30P_2O_5$ glasses were prepared by melt-quench method from sodium carbonate (Na_2CO_3), titanium trioxide (TiO_2), sodium tungstate Na_2WO_4 and hydrogen ammonium phosphate ($NH_4H_2PO_4$) purchased from Aldrich Chemicals. These precursors were weighed in a microanalytical balance and mixed thoroughly according to appropriate molar compositions. The mixture was first heated at 600°C for several hours in an alumina crucible. Then, the temperature is increased to attain the melt and was stirred for homogenization. The melt was then quenched to room temperature in air by pouring it on a preheated aluminum polished plate and pressing quickly by another one. The thin discs of glasses obtained in the above manner were transparent and colorless. Care was taken to see that the samples were not exposed to moisture, so they were placed in a desiccator before uses.

* *Corresponding author: E-mail: bihlahcen@yahoo.fr (Lahcen BIH)*

The amorphous state of all as-quenched samples was confirmed by powder X-ray diffractometry (XRD), using a Phillips D5000 apparatus equipped with a CuK_α X-ray source and a Ni filter (λ = 1.54 Å). No Bragg peaks were detected in a wide range of 2θ angles between 10° and 100°.

The density measurements (ρ) of glasses are determined by the Archimedes method using diethyl orthophthalate at 22 °C as the suspension medium. The uncertainty of the measurements is estimated to be $\pm$ 0.01 g/cm^3. Molar volume (V_m) of each glass is derived from the molar weight values (M) and the density (V_m=M/ρ).

The thermal stability of the studied glasses was studied by the Differential Scanning Calorimetric (DSC). DSC curves were carried out for ground glass batches of about 40 mg in nitrogen atmosphere at a heating rate 10°C/min using DSC131 Evo analyzer. The estimated error on the temperature is $\pm$ 4°C. Since the particle size of the ground glass batches can affect the shape of the DSC curves, we have used nearly the same particle sizes (glass powder passed through a 500 µm sieve but was retained over a 300 µm sieve) in all the determinations.

The local structure of the samples was examined by the Fourier transform infrared FTIR TENSOR27 spectrometer. FTIR absorption spectra of all glasses were recorded in the 400-1500 cm^{-1} frequency range at room temperature. For these measurements, each sample was ground to a fine powder, mixed with KBr in the ratio 1:100, and vacuum pressed into a disk.

UV–vis diffuse reflectance spectroscopy was performed on a Jasco v-570 spectrophotometer over the spectral range of 200–1200 nm. A barium sulfate ($BaSO_4$) plate was used as the standard (100% reflectance) on which the finely ground sample from the glass was coated.

Electrical measurements of the prepared glasses were performed by Impedance Spectroscopy (IS) Hewlett Packard Model 4284A precision LCR. The amplitude of the DC signal applied across the sample was 0.5 V. The glass pellets were coated with silver paint on either faces**.** The real and imaginary parts of the complex impedance were determined as a function of frequency [20Hz–1MHz] and temperature [328K – 627K].

3. Results and discussion

3.1. Glassy formation and XRD analysis

The glasses with the chemical compositions $20Na_2O$-$(50-x)Na_2WO_4$-$xTiO_2$-$30P_2O_5$ ($0 \le x \le 25$ mol %) were elaborated by the melt-quench route. The samples were free from visible inhomogeneities, such as inclusions, cracks or bubbles. The homogeneous samples could be elaborated up to 25 mol% of TiO_2. The structural nature of the elaborated samples is checked by X-ray diffraction analysis. XRD patterns for different samples (Fig.1) show only broad humps at low angles which confirm the amorphous nature of these samples. It is observed that some XRD patterns showed two to three humps. These multiple broad XRD have been confirmed to be related to the intermediate range order of the glass network [15]. The glasses were colorless suggesting that the transition metal ions are in their high valency states. In other words, the absence of reduced species W^{5+} and Ti^{3+} in the glass network is in agreement with the fact that the glasses containing the latter reduced species are colored blue or brown [16,17]. The glasses are also stable and non-hygroscopic at ambient temperature suggesting their water-resist nature.

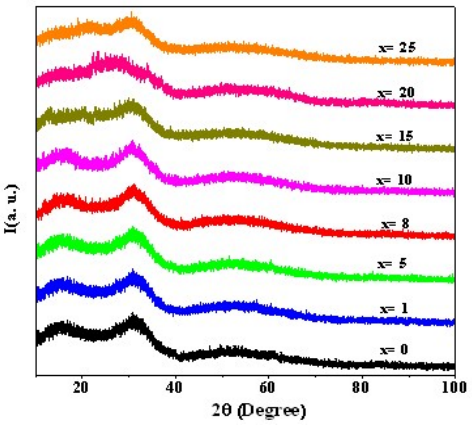

***Fig.1**. X-Ray patterns of the Na_2O-Na_2OWO_4-TiO_2-P_2O_5 glasses.*

3.2. Density and molar volume

Variations of the density and the molar volume as a function of the composition for the studied glasses are shown in Fig.2. With increasing TiO_2 content, it is observed that the density decreases while the molar volume increases. The determined values for these parameters are gathered in Table 1. The results show that the density decreased from 4.58 g/cm^3 (x=0) to 3.20 g/cm^3 (x=25). This decrease may be attributed to the large difference in molecular weight between Na_2WO_4 (293.83 g/mol) and TiO_2 (79.89 g/mol) which reveals that the introduction of lighter molecule in the glass instead of heavier ones decreases the density. The decrease in density indicates that the glass structure becomes less tightly packed with titanium oxide content.

From Table 1, one can observe that the molar volume changed from 44.09 cm^3 (x=0) to 46.37 cm^3 (x=25) when TiO_2 replaced Na_2WO_4. This increase of molar volume could be due to the change either in interatomic spacing or the stretching force constant of the bonds inside the glassy network. Practically, the increase of volume with (x) put forward that the interatomic spacing among the atoms of glass network increases when TiO_2 ratio goes up. Specially, the increase of the average length of M-O (M=P, W, Ti) bonds can explain the observed increase of (V_m). This happens when some bridging oxygen (BO) convert to non- bridging oxygen (NBO) in the glassy-matrix.

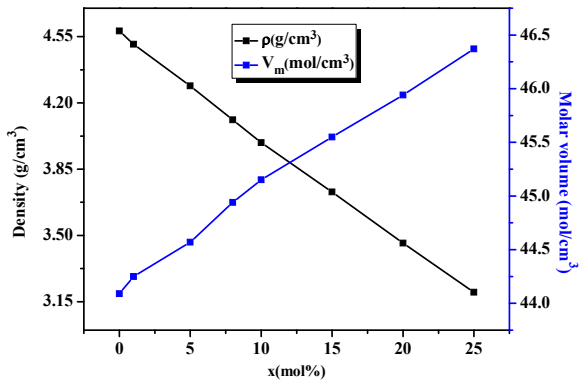

***Fig.2**. Composition dependence of the density and the molar volume for glasses.*

Table 1
Some physical properties for the studied glasses.

x (mol%)	Density (g/cm^3)	Molar volume (cm^3/mol)	OPD	T_g (°C)
0	4.58	44.09	83.93	405
1	4.51	44.25	83.08	420
5	4.29	44.57	84.91	423
8	4.11	44.94	82.18	442
10	3.99	45.15	79.68	428
15	3.73	45.55	79.88	433
20	3.46	45.94	77.35	480
25	3.20	46.37	74.59	493

3.3. DSC analysis

Fig.3 showed the DSC curves of the glasses which allow us to determine the glass transition temperature of the samples. Table 1 shows the determined values of Tg. Fig.4 represents the composition dependence of the glass transition temperature (T_g). The replacement of Na_2WO_4 by TiO_2 leads to an increase of T_g in the glass from 405 °C (x=0) to 493 °C (x=15). The glass transition temperature is well known to be a structural sensitive parameter depending on the bond strength, degree of cross-link density and closeness of packing [18]. According to the M-O (M=Ti, W) bond strength [19], the increase of Tg with TiO_2 amount is not due to the increase of the bond strength in the glasses since bond strength of Ti-O (≈666.5kJ / mol) is lower than that of W-O (≈720 kJ/ mol). In order to determine the effect of the oxygen packing density (OPD) on Tg, we have calculated this parameter and Fig.4 shows its variation versus TiO_2 content. From this latter figure, the (OPD) parameter could not explain the increase of Tg since it showed a decreasing behavior with titanium oxide in an opposite trend to that of the glass transition temperature. According to these two parameters we can assume that neither the bond strength nor the oxygen-packing density parameter controls the variation of T_g. The observed increase of T_g (Fig.4) could be due to an increase of the network connectivity or cross-link density due to TiO_x (x=4 or 6) structural units insertion in the phosphate glassy network. The insertion of titanium structural units between phosphate groups stimulates a polymerization of the glass network with a higher three-dimensionality and a resulting higher connectivity.

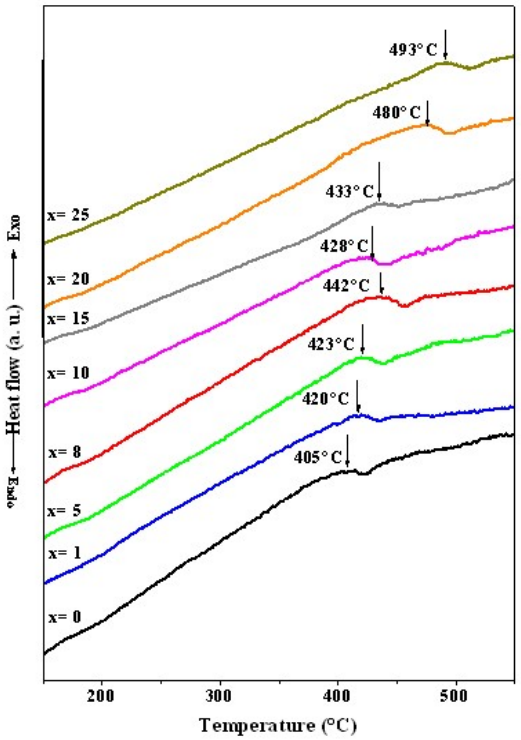

***Fig.3**. DSC curves of the studied glasses.*

As a result of this connectivity or reticulation the Tg value of the glass increases with TiO_2 content. From the chemical formulae of the glasses $20Na_2O$-(50-x)Na_2WO_4-xTiO_2-$30P_2O_5$ (0≤x≤25 mol %, we can visualize the substitution (50-*x*)Na_2WO_4-*x*TiO_2 as (50-*x*)Na_2O-*x*TiO_2 and (50-*x*)WO_3-*x*TiO_2 systems. From (50-*x*)Na_2O-*x*TiO_2 system one can deduce that the increase of T_g (Fig.4) is linked to the decrease of the modifier Na_2O content in the glasses.

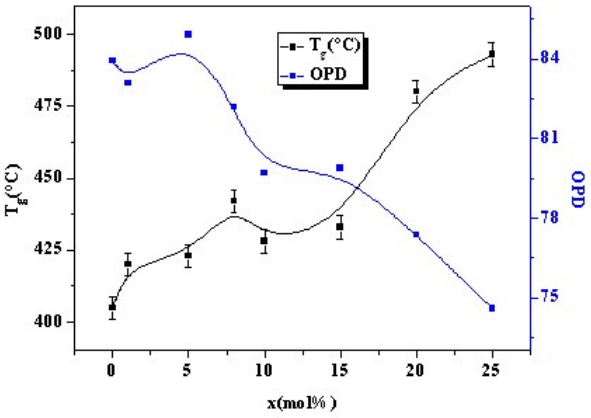

***Fig.4**. Glass transition temperature (Tg) and oxygen packing density (OPD) of the studied glasses.*

By analyzing the other (50-*x*)WO_3-*x*TiO_2 system and in order to form [TiO_6] octahedral units in the network, TiO_2 ($TiO_{4/2}$) must borrow oxygen from the glassy network. By taking off the oxygen atoms of the neighbor

phosphate networks, titanium has a strengthening effect on the structure when it substitutes tungsten. As a result of this cross-linking (reticulation), the rigidity of the glass skeleton increases which contributes concomitantly to the increase of T_g (Fig.4).

3.4. Infrared spectroscopy

The IR spectra of the studied glasses in the frequency range 400 cm^{-1}-1400 cm^{-1} are shown in Fig.5. According to the literature [20], the assignments of the different bands are given in Table 2. The asymmetric stretching vibrational of P=O bond (ν_{as}(P=O)) and/or $\nu_{as}(PO_2)^-$, in metaphosphate units often called Q^2, units appear as a broad weak band in the range 1220-1200 cm^{-1}. The band near 1160 cm^{-1} has been assigned to symmetric stretching modes, $\nu_s(PO_2)^-$ of metaphosphate chains. The strong band at 1100 cm^{-1} is attributed to asymmetric stretching modes, $\nu_{as}(PO_3)^{2-}$, of pyrophosphate groups. The weak band at 1070 cm^{-1} is assigned to symmetric stretching mode of $(PO_3)^{2-}$ units. The low intense shoulder at 1040-1000 cm^{-1} is assigned to orthophosphate PO_4^{3-} groups. The band at 970-930 cm^{-1} is attributed to the asymmetric vibrations, ν_{as}(P–O–P) and/or ν_{as}(P–O–M)(M=W, Ti). The band at 730-720 cm^{-1} may be attributed to symmetric stretching vibrations, ν_s(P–O–P), of bridging oxygen atoms. The broad bands in the range 500-480 cm^{-1} belong to the bending vibrations of basic structural units of phosphate glasses. The motion mode of sodium species is located in this latter frequency range.

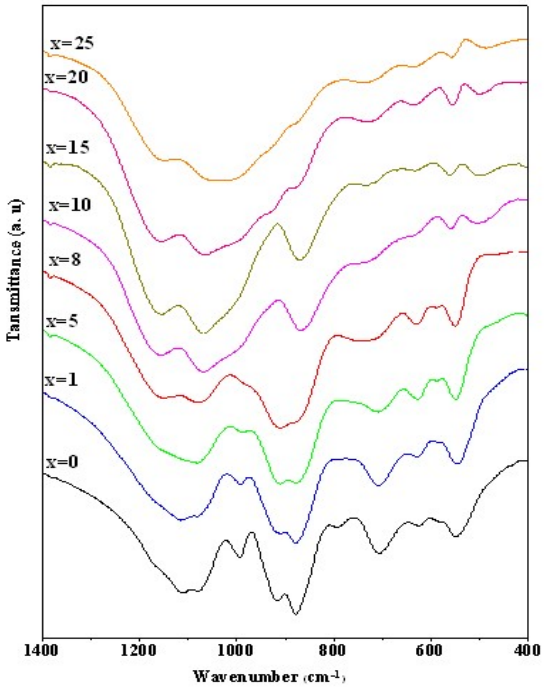

***Fig.5**. Infrared spectra of the studied glasses.*

From the analysis of the spectra, it is seen that the Ti-W substitution inside the glasses under study induces some changes in the shape and the intensity of some IR bands. In the IR spectrum of the glass containing tungsten only, it is seen the coexistence of WO_4 (880 cm^{-1}) and WO_6 (950 cm^{-1}) groups [21-23]. With the increase of TiO_2 content in the glasses, the intensities of the vibration modes associated to some phosphate units and (WO_4) units become weak while the intensities of the shoulders near 725 cm^{-1} and 640 cm^{-1} increase. The latter bands are ascribed to Ti-O-Ti symmetric stretching vibrations of TiO_4 units and the vibrations of TiO_6 structural units [24], respectively. Generally, we can conclude that the increase of TiO_2 content in the glass induces an increase of the intensity of bands related to metaphosphate structural units, $(PO_2)^-$ and P-O-P bands while the intensity of band due to pyrophosphate structural groups,$(PO_3)^{2-}$, decreases.

Table 2
IR band assignments in the 400-1400 cm^{-1} frequency range for the studied glasses.

Position of band (cm^{-1})	Band assignment
1240	ν_{as}(P=O)/$\nu_{as}(PO_2^-)$
1160	$\nu_s(PO_2)^-$
1100	$\nu_{as}(PO_3)^{2-}$
935-920	ν_{as}(P-O-P)/ ν_{as}(P-O-M) (M= W, Ti)
880-870	MO_6 (M= W, Ti)
735	ν_s(P-O-P)
725	(TiO_4)
640-630	ν_s(M-O-M) (M= W, Ti)
500-425	δ(O-P-O) / translation of cations

3.5. Optical properties

The optical absorption spectra of the glasses under study are given in Fig.6. All the absorption curves are characterized by a broad onset of absorption edge over the region of 200-450 nm. This UV absorption edge originates from an electron transition between oxygen 2p and transition metal ion 3d states [25]. The onset of the absorption depends on the chemical composition of the glasses. With substitution of Na_2WO_4 by TiO_2, it is observed that: (i) this onset is red shifted; (ii) there is no absorption in the region 400-700 nm. According to the fact that Ti^{3+}or W^{5+} ions in glass are characterized by an absorption in the visible region around 500-800 nm [26], one can state that the glasses under study are free from reduced species of titanium (Ti^{3+}) and tungsten (W^{5+}). Indeed, the colorless of the glasses confirms that the formation of Ti^{3+} species is unlikely in these samples.

The optical band gap (E_g) of a glass is obtained from the absorption coefficient α(ν) in the ultraviolet absorption edge [27, 28]. The variation of $(\alpha h\upsilon)^{1/2}$ as a function of hυ (known as a Tauc plot) is used to determine E_g value in optical data of the glass. Fig.7 represents the Tauc plots of the glasses and the obtained values of E_g are gathered in Table 3. From these data one can see that the gap energy decreases with increasing TiO_2 content in the glass. For the glass (x= 0), the value is found to be 2.92 eV. The (5 mol %) substitution of Na_2WO_4 by TiO_2 results in reduced E_g

value to 2.45 eV. For the glasses (x=8) and (x=10), the values of E_g are 2.27eV and 2.05eV, respectively. Further slight reduction in E_g value (1.73 eV) is noted for the glass (x=25). This decrease of E_g could be explained by the increase of the non-bridging oxygen (NBO) ions in the glasses owing to the insertion of TiO_2 in the network.

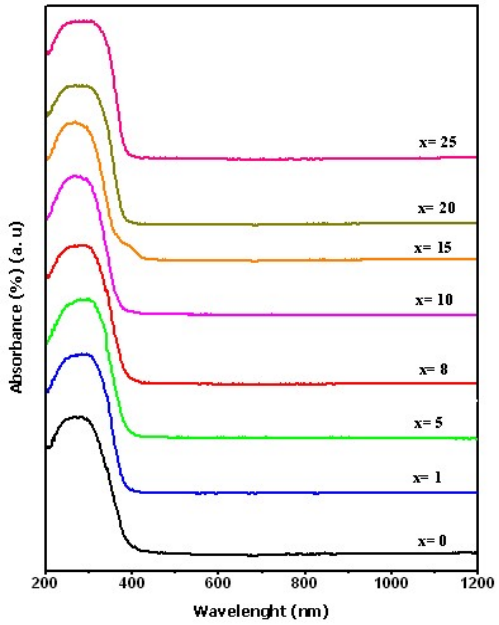

***Fig.6**. Optical absorption spectra of the prepared glasses*

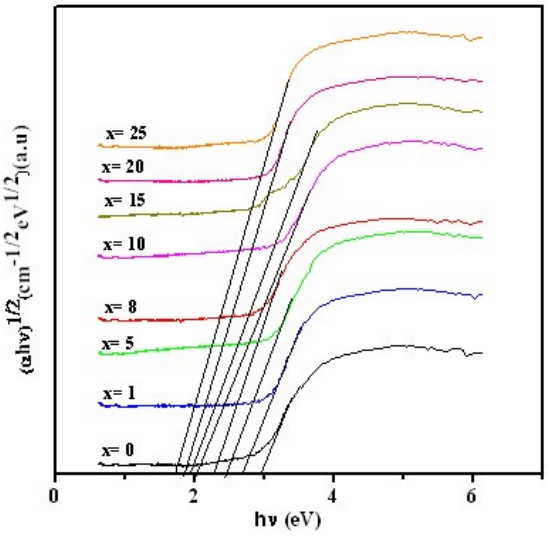

***Fig.7**. Variation of $(\alpha h\upsilon)^{1/2}$ as a function of (hυ for studied glasses.*

In order to estimate the degree of the disorder induced by the substitution of W by Ti in the glasses, we have explored the region of lower photon energy of the edge for the glasses. In this region the absorption coefficient changes into an exponential dependence, as given by the Urbach law [29]. The absorption coefficient α(v) depends exponentially on the photon energy (hv). The exponential dependence known as the Urbach rule [29] may be written in the form:

$$\alpha(v) = B \exp(h\nu/\Delta E) \quad (1)$$

where B is a constant and ΔE is the width of the band tails of the localized states in the band gap. The plots of ln(α) versus hν of the glasses are represented in Fig.8. From a linear plot for certain region of absorption coefficient the values of the Urbach energy ΔE can be calculated and are given in Table 3. With increasing Ti/W ratio in the glass the Urbach energy increases suggesting the increase in structural disorder of glasses as the amount of TiO_2 increased (Fig.9).

Table 2

Optical band gap and Urbach energy of the fundamental optical band for studied glasses.

x (mol%)	Optical band gap E_{opt}(eV)	Urbach Energy ΔE (eV)
0	2.92	0.41
1	2.67	0.42
5	2.45	0.44
8	2.27	0.48
10	2.05	0.53
15	1.93	0.57
20	1.84	0.60
25	1.73	0.64

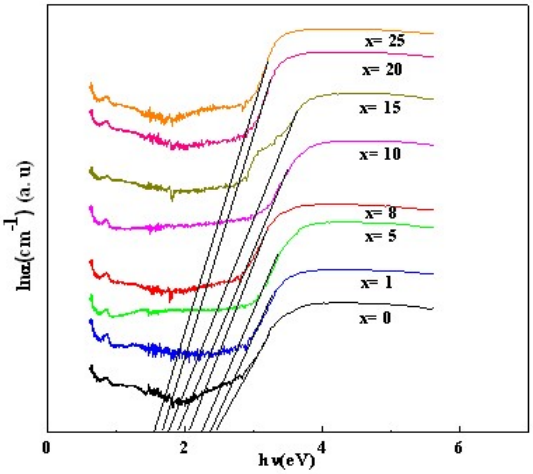

***Fig.8**. Variation of ln(α) as a function of* hυ *for the prepared glasses.*

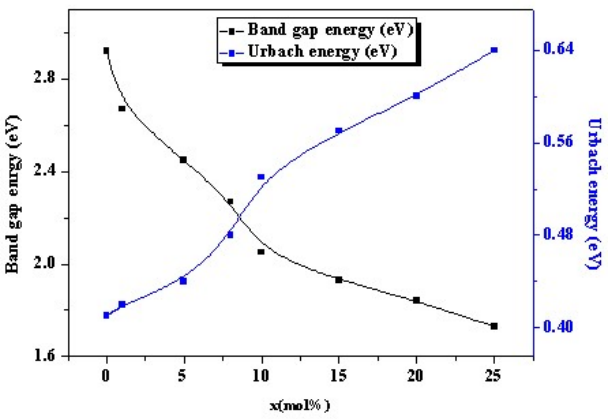

***Fig.9**. Variation of band gap energy and Urbach energy as a function of TiO_2 content.*

3.6 Electrical properties

The conductivity of each glass was calculated using the bulk resistance obtained from the analyzed impedance data and pellet dimensions according to the following equation:

$$\sigma = (t/a)*(1/Z) \quad (2)$$

where σ is the conductivity, 't' is the thickness, 'a' is cross-section area of the pellet and 'Z' is the bulk resistance.

The variation of the conductivity as a function of temperature is shown in Fig.10. From this latter, we deduced that the temperature dependence of conductivity for the prepared glasses followed an Arrhenius behavior:

$$\sigma.T = \sigma_0 \exp(-E_a/k_BT) \quad (3)$$

where, E_a is the activation energy for conduction, σ_o is the pre-exponential term and k_B is the Boltzmann constant.

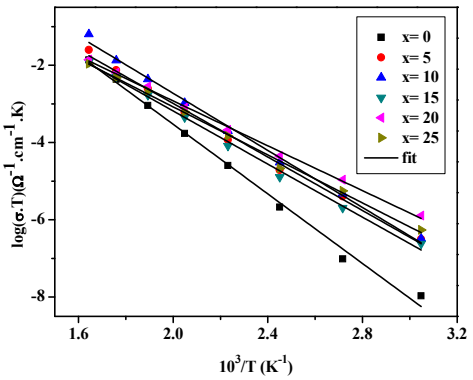

***Fig.10**. log(σ$_{dc}$.T) vs 1000/T plots for the prepared glasses.*

The determined values of 'log σ' at 408K, log σ_0 and E_a are listed in Table 4. Generally, it is found that the dc conductivity increases with TiO_2 content in the glasses. This increase is accompanied with a decrease of the activation energy. Since the prepared glasses are colorless one can suppose that the contribution of electronic conduction to the total conductivity is negligible or very low. Therefore, the conductivity of the studied glasses is due to the sodium ions.

In order to determine some parameters of the conduction in the glasses, the conductivity data are analyzed by the modulus formalism (M=M'+iM"). The real and imaginary parts of (M) calculated from the measured impedance data are given by equations (4) and (5):

$$M' = \omega C_0 Z'' \quad (4)$$

$$M'' = \omega C_0 Z' \quad (5)$$

where, Z′ and Z″ are the real and imaginary parts of the impedance, respectively. ω is the angular frequency and C_0 is the vacuum capacitance of the cell.

The variation of the imaginary component of modulus M″/M″$_{max}$ as a function of frequency at different temperatures provides more information related to charge transport processes such as mechanism of electrical transport. The M″/M″$_{max}$ spectra for different compositions showed a slightly asymmetric peak at each temperature. The frequency range below the peak frequency f_p determines the range in which charge carriers are mobile over short distances [30]. Moreover, the asymmetric nature of M″/M″$_{max}$ spectra suggested that the relaxation present in the material was non-Debye. Fig.11 showed the imaginary part of the electric modulus M″/M″$_{max}$ as a function of frequency at several temperatures for the glasses (x=0 and x=10). The maximum in the M″/M″$_{max}$ peak shifts to higher frequency with increasing temperature. The shift in M″/M″$_{max}$ peak maximum corresponds to the conductivity relaxation. This behavior suggests that the dielectric relaxation is thermally activated. In order to determine the mechanism of the conduction, we have plotted the variation of the frequency associated with the maximum of M" as a function of temperature. For each glass, we found that this variation followed an Arrhenius behavior with activation energy (E_f). In Fig.12 we showed the obtained results for the glasses (x=5 and x=20). In the same figure we plotted the temperature dependence of the conductivity. Both lines are quasi-parallel and the activation energies issued from impedance (E_a) and modulus (E_f) spectra are very similar (Table 4). This result suggests that the electrical conductivity in the glasses under study is probably due to a hopping mechanism [31].

Table 4

Electrical parameters of the studied glasses.

X (mol %)	logσ$_{dc}$.408 (Ω^{-1}.cm^{-1}.K)	E_a(eV)	E_f(eV)	β
0	-8.29	0.89	0.90	0.64
5	-7.33	0.69	0.69	0.66
10	-7.60	0.73	0.72	0.71
15	-7.51	0.68	0.68	0.52
20	-6.96	0.58	0.57	0.51
25	-7.28	0.62	0.62	0.46

The asymmetric nature of M″/M″$_{max}$ spectra suggested that the relaxation behavior was non-Debye and could be characterized by the stretched exponent parameter β < 1 [32]. For an ideal dielectric material, for which the dipole–dipole interaction is negligible, the value of β is equal to unity (β = 1). The stretched exponent parameters, β, can be obtained from the peak relaxation frequency (β = 1.14/FWHM), where (FWHM) is the width at half-maximum of M''(f) curves. For each glass, it is found that the value of β is independent of temperature and the obtained values of β for all the compositions are regrouped in Table 4. The values of β are found to be less than unity. This demonstrated the non-Debye nature of the dielectric relaxation inside the glasses.

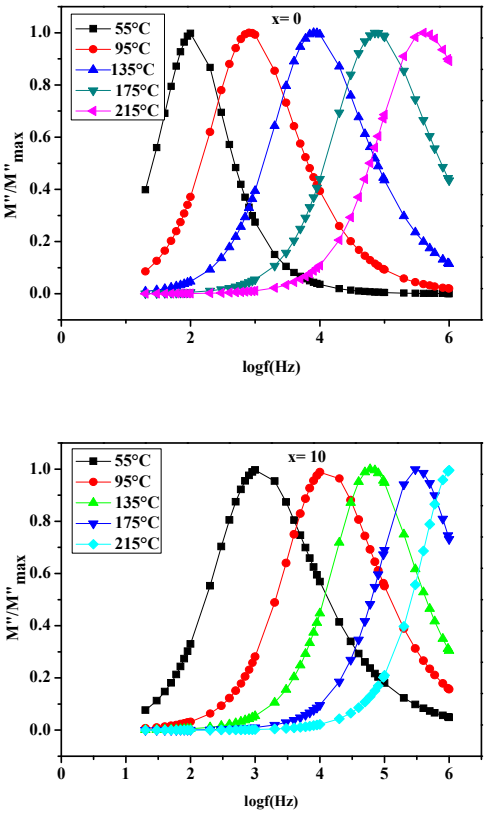

***Fig.11**. M"/M"$_{max}$ dependence of frequency for the glasses (x= 0) and (x=10).*

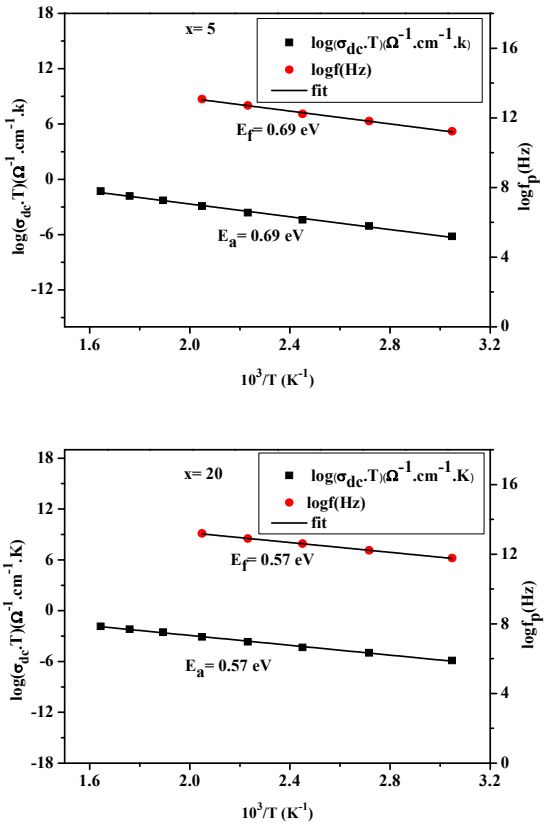

***Fig.12**. Temperature dependence of logσdc.T and logfp for the glasses (x= 5) and (x=20).*

4. Conclusion

The colorless glasses inside the $20Na_2O$-(50-x)Na_2WO_4-xTiO_2-$30P_2O_5$ (0≤x≤25 mol%) system were prepared by melt-quenching route. With the increase of Ti/W ratio, it is found that the glass transition temperature (T_g) increases due to the reticulation effect of TiO_2 in the network. IR spectra indicate the formation of different structural units and the content of metaphosphate groups goes up when TiO_2 substitutes Na_2WO_4. The variations of optical band gap and Urbach energy depend on the glass composition. It is observed that the increase of Ti/W ratio in the glass induces a decreasing of the gap energy value while the disorder degree increases. The electrical conductivity of the glasses is mainly due to the Na^+ ions and it increases with Ti/W ratio. The Na^+ charge transfer in the studied glasses is due to the hopping mechanism and the dielectric relaxation inside the glasses is non-Debye nature.

Acknowledgments

The authors would like to thank the Swedish Research Council for the financial grant SRL(MENA) # 348- 2014-4287. Lahcen BIH is also grateful to the CNRST for their support in the framework of PPR project (ENERGYPHOS).

References

[1] B. C. Sales, L. A. Boatner, Journal of Non-Crystalline Solids 79 (1986) 83-116.
[2] Y. B. Peng, D. E. Day, Glass Technology 32 (1991) 166-173.
[3] G. Fuxi, Journal of Non-Crystalline Solids 123 (1990) 385-399.
[4] L. D. Bogomolova, Journal of Non-Crystalline Solids 30 (1979) 379-383.
[5] S. Krimi, A. El Jazouli, L. Rabardel, M. Couzi, I. Mansouri, G. Le Flem, Journal of Solid State Chemistry 102 (1993) 400-407.
[6] K. Brow Richard, R. David Tallant, Journal of Non-Crystalline Solids 222 (1997) 396-406.
[7] D. K. Sardar, J. B. Gruber, B. Zandi, J. A. Hutchinson, C. W. Trussell, Journal of Applied physics 93 (2003), 2041-2046.
[8] K. Franks, V. Salih, J. C. Knowles, I. Olsen, Journal of Materials Science 13 (2002) 549-556.
[9] M. Navarro, M. P. Ginebra, J. Clément, M. Salvador, A. Gloria, J. A. Planell, Journal of the American Ceramics Society 86 (2003) 1345-1352.
[10] L. Koudelka, P. Mos, J. Pospís, L. Montagne, G. Palavit, Journal of Solid State Chemistry 178 (2005) 1837-1843.
[11] H. Sinouh, L. Bih, A. El Bouari, M. Azrour, B. Manoun, P. Lazor, Journal of Non-Crystalline Solids 405 (2014) 33-38.
[12] M. A. Valente, L. Bih, M. P. F. Graça, Journal of Non-Crystalline Solids 357 (2011) 55-61.
[13] H. Es-soufi, L. Bih, B. Manoun, P. Lazor, Journal of Non-Crystalline Solids 463 (2017) 12-18.
[14] H. Es-Soufi, L. Bih, B. Manoun, D. Mezzane, P. Lazor, Materials Research Forum 04-06 (2016) 266-269.
[15] J.J. Cheng, Journal of Materials Science 16 (1981) 2531-2543.

[16] D. Boudlich, L. Bih, M. E. H. Archidi, M. Haddad, A. Yacoubi, A. Nadiri, B. Elouadi, Journal of the American Ceramics Society 85 (2002) 623-630.
[17] H. Sinouh, L. Bih, M. Azrour, A. El Bouari, S. Benmokhtar, B. Manoun, B. Belhorma, T. Baudin, P. Berthet, R. Haumont, D. Solas, Journal of Physics and Chemistry of Solids 73 (2012) 961-96.
[18] N. H. Ray, Journal of Non-Crystalline Solids 15 (1974) 423-434.
[19] D. R. Lide, CRC Handbook of Chemistry and Physics 82 Ed., CRC Press, 2001.
[20] H. Sinouh, L. Bih, B. Manoun, P. Lazor, Journal of Thermal Analysis and Calorimetry 128 (2017) 883-890.
[21] D. J. Geraci, J. E. Shelby, Journal of the American Ceramic Society 67 (1984) 654-657.
[22] T. Sekiya, N. Mochida, S. Ogawa, Journal of Non-Crystalline Solids 176 (1994) 105-115.
[23] B. V. R. Chowdari, K. L. Tan, L. Fang, Journal of solid state ionics 136 (2000) 1101-1109.
[24] G. Laudisio, M. Catauro, A. Aronne, P. Pernice, Thermochimica acta 294 (1997) 173-178.
[25] B. S. Bae, M. C. Weinberg, Journal of Applied physics 73 (1993) 7760-7766.
[26] T. Hashimoto, H. Nasu, K. Kamiya, Journal of the American Ceramic Society 89 (2006) 2521–2527.
[27] P. Nachimuthu, P. Harikishnan, R. Jagannatha, Physivs and Chemistry of Glasses 38 (1997) 59-62.
[28] E. A. Davis, N. Mott, Philosophical Magazine 22 (1970) 0903-0922.
[29] F. Urbach, Physical Review 92 (1953) 1324-1324.
[30] P. Ganguly, A. K. Jha, Physica B Condensed Matter, 405 (2010) 3154-3158.
[31] A. A. Bahgat, Journal of Non-Crystalline Solids 226 (1998) 155-161.
[32] M. H. Bhat, M. Ganguli, K. J. Rao, Bulletin of Materials Science 26 (2003) 407-413.